

Cancer Research

Identification of Cyclin D1– and Estrogen-Regulated Genes Contributing to Breast Carcinogenesis and Progression

Chuanwei Yang, Sally Trent, Viviana Ionescu-Tiba, et al.

Cancer Res 2006;66:11649-11658. Published online December 18, 2006.

Updated Version

Access the most recent version of this article at:
doi:[10.1158/0008-5472.CAN-06-1645](https://doi.org/10.1158/0008-5472.CAN-06-1645)

Supplementary Material

Access the most recent supplemental material at:
<http://cancerres.aacrjournals.org/content/suppl/2006/12/19/66.24.11649.DC1.html>

Cited Articles

This article cites 49 articles, 18 of which you can access for free at:
<http://cancerres.aacrjournals.org/content/66/24/11649.full.html#ref-list-1>

Citing Articles

This article has been cited by 7 HighWire-hosted articles. Access the articles at:
<http://cancerres.aacrjournals.org/content/66/24/11649.full.html#related-urls>

E-mail alerts

[Sign up to receive free email-alerts](#) related to this article or journal.

Reprints and Subscriptions

To order reprints of this article or to subscribe to the journal, contact the AACR Publications Department at pubs@aacr.org.

Permissions

To request permission to re-use all or part of this article, contact the AACR Publications Department at permissions@aacr.org.

Identification of Cyclin D1- and Estrogen-Regulated Genes Contributing to Breast Carcinogenesis and Progression

Chuanwei Yang,¹ Sally Trent,⁵ Viviana Ionescu-Tiba,² Lan Lan,³ Toshi Shioda,¹ Dennis Sgroi,⁶ and Emmett V. Schmidt^{4,6}

¹Massachusetts General Hospital Cancer Research Center; ²Department of Family Medicine, Boston University Medical Center; ³Molecular Biology and ⁴The Pediatric Service, Massachusetts General Hospital, Boston, Massachusetts; ⁵Department of Radiotherapy, Royal Marsden Hospital, London, United Kingdom; and ⁶Molecular Pathology Unit, Massachusetts General Hospital-East, Charlestown, Massachusetts

Abstract

Tumors can become lethal when they progress from preinvasive lesions to invasive carcinomas. Here, we identify candidate tumor progression genes using gene array analysis of preinvasive and invasive tumors from mice, which were then evaluated in human cancers. Immediate early response protein IEX-1, small stress protein 1 (HSPB8), and tumor necrosis factor-associated factor-interacting protein mRNAs displayed higher expression levels in invasive lesions than in preinvasive lesions using samples obtained by laser capture microdissection (LCM) from transgenic *erbB2*, *ras*, and *cyclin D1* mice. LCM-isolated tissues from patient-matched normal, ductal carcinoma *in situ*, and invasive ductal carcinoma revealed similar increased expression in invasive human cancers compared with preinvasive and normal samples. These genes induced anchorage independence, increased cell proliferation, and protected against apoptosis, singly or in collaboration with *erbB2*. Surprisingly, they were all up-regulated by 17 β -estradiol and cyclin D1, and cyclin D1 overexpression increased p300/CBP binding to their promoters, supporting the model that cyclin D1-estrogen receptor (ER) coactivator interactions may be important to its role in ER-positive breast cancer. Additionally, an irreversible dual kinase inhibitor of ErbB signaling inhibited expression of the same genes. The up-regulation of genes contributing to increased invasiveness of ER-positive cancers offers a novel explanation for the contribution of cyclin D1 to a worse prognosis in ER-positive cancers. As targets of estrogen, cyclin D1, and *erbB2* signaling, these candidates offer insights into the nature of the second events involved in breast cancer progression, regulatory events contributing to invasion, and potential targets of combined inhibition of hormone and growth factor signaling pathways. (Cancer Res 2006; 66(24): 11649-58)

Introduction

Human malignancies are highly evolved and complex tissues that result from selection for mutations that permit autonomous growth (1). Tumors can become lethal when they locally invade or distantly metastasize; both events define tumor progression (2).

Note: Supplementary data for this article are available at Cancer Research Online (<http://cancerres.aacrjournals.org/>).

Requests for reprints: Emmett V. Schmidt, Massachusetts General Hospital Cancer Research Center, Massachusetts General Hospital Cancer Center-Harvard University, 55 Fruit Street, GRJ 904, Boston, MA 02114. Phone: 617-726-5707; Fax: 617-726-4466; E-mail: schmidt@helix.mgh.harvard.edu.

©2006 American Association for Cancer Research.
doi:10.1158/0008-5472.CAN-06-1645

The long-dominant model of tumor progression considers it the result of individual stochastic mutations that accumulate in progressively more aggressive subpopulations (3). A more recent view proposes that tumor progression results from continuous selection for events that originally caused the tumor, which become quantitatively more abnormal (4–6). This alternative model is particularly supported by laser capture microdissection (LCM) studies of disease progression (5, 7). Because much of our knowledge of the pathologic stages of breast cancer is based on histologic observations and it is critical to define events that take place in specific cell populations, LCM is a particularly attractive approach to evaluate genetic changes accompanying tumor progression.

We addressed previously this issue by examining tumor progression in humans using LCM-dissected tissues from patients who had been diagnosed with both noninvasive and invasive tumors (5). Mouse models that recapitulate tumor progression offer an attractive alternative for analysis (8). Early transgenic studies focused on the stochastic nature of tumor development in transgenic models (9). In contrast, quantitative, nonstochastic expression changes accompanying transgenic tumor progression have received little attention. Identification of conserved genetic events accompanying tumor progression in both mouse models and human disease should provide a powerful approach to genetic analysis of tumor progression.

Cyclin D1 remains a particularly interesting breast cancer oncogene (10). Its expression is both essential for normal mammary development and its overexpression causes mammary tumors (11, 12). Cyclin D1 acts either by associating with cyclin-dependent kinases (CDK) 4/6 to phosphorylate the retinoblastoma protein (pRb; ref. 13), by titrating p21-CIP1 away from other G₁-regulating CDKs (14), or by CDK-independent transcriptional effects (15). Overexpression of cyclin D1 is associated with estrogen receptor (ER)-positive breast cancers and connotes a worse prognosis (16–19). This has been explained variously as resulting from estrogen regulation of cyclin D1 (20) or as the result of direct interactions between ER coactivators and cyclin D1 that activate estrogen response elements (ERE; refs. 21–23). However, no endogenous gene has been identified that responds to both cyclin D1 and estrogen as predicted by these protein-protein interactions, and no estrogen-responsive gene has been associated with invasive breast cancers caused by cyclin D1.

Tumors develop in cyclin D1-overexpressing mammary models following a long preinvasive phase (24). Accumulating genetic evidence also places cyclin D1 as a downstream effector of tumor formation by *erbB2* (25, 26). Tumors in *erbB2* transgenic mice show increased cyclin D1 levels; this increase is mediated by *ras* signaling. Consequently, increased cyclin D1 expression is expected in mouse mammary tumor virus (MMTV)-*erbB2*, MMTV-*ras*, and

MMTV-cyclin D1 transgenic tumors (27). The coexistence of invasive tumors and large amounts of preinvasive tissue in mice from identical genetic backgrounds offers an interesting opportunity to evaluate quantitative genetic events accompanying breast cancer progression.

Here, we report the identification of candidate tumor progression genes in oncogene-specific breast cancer models that were then evaluated in human tumors for parallel quantitative changes associated with disease progression. We focused on breast tumors induced by *erbB2* and *cyclin D1* because these genes are clinically important and may lie in the same signaling pathway (11, 25). Using this approach, we identified three genes associated with cancer progression that blocked apoptosis and promoted oncogenic transformation in cell-based models. Expression of all three genes increased in response to cyclin D1 and estrogen, providing an interesting new explanation for the known association between cyclin D1 expression and poor prognosis, ER-positive breast cancers.

Materials and Methods

Cell culture and DNA constructs. MCF-7, BT-474, MDA-MB-453, and NIH3T3 cells were grown in conditions indicated by the supplier (American Type Culture Collection, Manassas, VA). The IEX-1 vector was from S. Maheswaran [Massachusetts General Hospital (MGH), Boston, MA], the 17 β -estradiol-inducible small stress protein (SSP) 1 (E2-SSP1, HSPB8, HSP22) plasmid was from R. Benndorf (University of Michigan, Ann Arbor, MA), and the tumor necrosis factor (TNF)-associated factor-interacting protein (TRAF-IP) plasmid was from S. Lee (Rockefeller University, New York, NY). The pRC-CMV-cyclin D1 was from Dr. Rolf Muller (Institut für Tumorforschung, Marburg, Germany; ref. 28), and LALA and KE mutant cyclin D1s were from Dr. Rene Bernards (Netherlands Cancer Institute, Amsterdam, the Netherlands; refs. 22, 23).

Mice, tumor samples, and LCM. MMTV-cyclin D1 and MMTV-erbB2 transgenic mice were described previously (25). MMTV-ras mice were purchased from Charles River Laboratories (Wilmington, MA). Female transgenic mice were maintained in inbred FVB genetic backgrounds according to approved protocols of the MGH Animal Advisory Committee. LCM was described previously (5). For transgenic mouse samples, tumors or preinvasive mammary tissues were simultaneously microdissected from the tumors and a contralateral uninvolved gland.

LCM, RNA isolation and amplification, microarray analysis, human samples, and quantitative real-time PCR analysis. For mouse samples, total RNA was extracted from captured cells and underwent two rounds of T7-based RNA amplification (5). The amplified RNA (aRNA) product was converted to double-stranded cDNA, which was used for probe synthesis in microarray analysis containing 5,184 murine cDNAs (Research Genetics, Carlsbad, CA) as described (5).

For human samples, patient-matched normal breast tissue, atypical ductal hyperplasia (ADH), ductal carcinoma *in situ* (DCIS), or invasive ductal carcinoma (IDC) were microdissected from snap-frozen breast tissue where the normal tissue was at a minimum 0.3 cm from any premalignant or malignant lesion. The clinical characteristics of the 36 patients used in these studies are described in previous Supplementary Materials (5).⁷ Both ADH and DCIS were available for seven of these patients and are summarized together as DCIS-ADH in our data below ($n = 42$). IDC samples were available from 27 of the patients. For both mouse and human samples, quantitative real-time PCR (qRT-PCR) was done using standard methods (25). Primer sets used are listed in Supplementary Table S1.

To validate the human genes identified by the LCM-isolated patient samples, we evaluated an alternative set of paired bulk tumor-normal samples (29). Sufficient material was available from nine patients to isolate mRNA and analyze it by qRT-PCR.

Western blot analysis. For Western blots, frozen mammary tissues were crushed in liquid nitrogen using a mortar and pestle. Protein lysates were made by passing the resulting powders through a 20-gauge needle at 4°C in TNE buffer [50 mmol/L Tris (pH 8.0), 150 mmol/L NaCl, 5 mmol/L EDTA, 1% NP40]. Fifty microgram of total protein were used in standard immunoblots. Membranes were incubated with an affinity-purified rabbit polyclonal anti-cyclin D1 (16), rabbit polyclonal anti-erbB2 (A0485, DAKO, Carpinteria, CA), and two anti-ER antibodies (HC-20 and MC-20, Santa Cruz Biotechnology, Santa Cruz, CA). A mouse monoclonal antibody against actin (Boehringer, Ridgefield, CT) assessed loading equivalence. Secondary antibodies were either purchased from Santa Cruz Biotechnology or those included in an enhanced chemiluminescence detection kit (Amersham, Piscataway, NJ).

Soft agar colony formation assay. For NIH3T3 soft agar assays, NIH3T3 cells were stably transfected; pools of transfectants were selected in G418, and these pools were used in soft agar assays (30). For MCF-10A soft agar assays, cells expressing an erbB2 chimera were infected with pBabe-puro retroviruses containing the genes of interest (31), and pools of cells selected in puromycin were used for soft agar assays.

erbB2 dimerization. Inducible activation of erbB2 was carried out using a chimeric form of erbB2, which contains the extracellular and transmembrane domains from the p75 low-affinity nerve growth factor receptor, the cytoplasmic domain of erbB2, and the FKBP ligand binding domain (32). Cells expressing the chimera were treated with the synthetic FKBP analogue AP1510 (500 nmol/L; Ariad, Boston, MA) to inducibly activate erbB2 (31, 32).

3-(4,5-Dimethylthiazol-2-yl)-2,5-diphenyltetrazolium bromide assay. MCF-7, BT-474, or T47D cells stably transfected with genes of interest were seeded at a density of 1,000 per well for 10 wells per cell construct per time point in a 96-well plate and cell numbers or proliferation were assayed with 3-(4,5-dimethylthiazol-2-yl)-2,5-diphenyltetrazolium bromide (MTT; ref. 33). One-way ANOVA and/or Student's *t* test were used to determine statistical significance.

Apoptosis analysis by Z-Val-Ala-Asp-fluoromethyl-ketone assay. Because MCF-7 cells lack caspase-3, a cell-permeable tripeptide [Z-Val-Ala-Asp-fluoromethyl-ketone (Z-VAD-fmk)] that broadly inhibits multiple caspases was used to assess apoptosis (34). MCF-7 cells were seeded at 200,000 per well in a six-well plate. Cells grown to 70% confluence were incubated with 50 μ mol/L Z-VAD-fmk or vehicle control for 1 hour before the addition of 10 ng/mL TNF- α or its vehicle. For growth factor removal-induced apoptosis, cells grown to 75% confluence were incubated in phenol red-free and serum-free medium for up to 6 days. Apoptosis was monitored daily beginning 3 days after serum removal. Seventy-two hours after TNF- α treatment or at the end of growth factor removal, the attached cells were trypsinized and mixed with the floating cells in the cell medium. Trypan blue-excluding cells were counted using a hemocytometer. Apoptosis was determined as the difference between trypan blue-stained cells treated with vehicle and those treated with Z-VAD-fmk.

Measurement of gene regulation by estrogen and cyclin D1. The estrogen dose-response assay was conducted using MCF-7 BUS cells (35) grown in the indicated concentrations of 17 β -estradiol for 3 days; RNA was harvested during active proliferation. Levels of the indicated genes were measured using qRT-PCR and plotted as fold change. Each treatment was done in triplicate; mean and SDs are shown.

MCF-7 transfectants were created using cytomegalovirus (CMV)-driven vectors containing cyclin D1 or one of the two cyclin D1 mutants using G418 selection for colinear neomycin markers. Proliferating MCF-7 cells expressing the cyclin D1 variants or empty vector control were incubated in phenol red-free DMEM with 5% charcoal-stripped serum for 3 days before treatment. Stable transfectants were then treated for 1 hour with 100 nmol/L 17 β -estradiol or vehicle control at 37°C and total RNA was harvested with Trizol (Invitrogen, Carlsbad, CA). mRNA was reverse transcribed into cDNA and converted to dsDNA. qRT-PCR was done as described above to assess response to 17 β -estradiol and/or the effects of overexpressed cyclin D1 or its mutants on gene expression.

Chromatin immunoprecipitation assays. We evaluated promoter binding in MCF-7 cells grown in phenol red-free DMEM with 5%

⁷ <http://www.pnas.org/cgi/content/full/100/10/5974>.

charcoal-stripped serum for 3 days and treated with vehicle or 100 nmol/L 17 β -estradiol for 1 hour. Cross-linking was done by adding 37% formaldehyde to a final concentration of 1.5% for 15 minutes at 25°C with gentle agitation. The reaction was stopped by adding 0.125 mol/L glycine for 5 minutes. Cells were scraped and collected by centrifugation; the pellet was washed twice with ice-cold PBS [120 mmol/L NaCl, 2.7 mmol/L KCl, 10 mmol/L phosphate buffer (pH 7.4)] and twice with immunoprecipitation buffer [150 mmol/L NaCl, 5 mmol/L EDTA, 1% Triton X-100, 0.5% NP40, 50 mmol/L Tris-HCl (pH 7.5), 0.5 mmol/L DTT] and resuspended with immunoprecipitation buffer supplemented with 0.5% SDS and protease inhibitor cocktail (Roche, Basel, Switzerland). Sonication was done until desired DNA fragment sizes were reached. The lysate was then subjected to 12,000 \times *g* centrifugation for 10 minutes. The supernatant was collected and diluted 5-fold with immunoprecipitation buffer. For immunoprecipitation, anti-ER antibody (HC-20), anti-p300/CBP antibody (A-22) from Santa Cruz Biotechnology, or an equal concentration of normal rabbit serum was added to the lysate and incubated at 4°C overnight with agitation. Protein A-Sepharose beads (Amersham) were added to the mixture and incubated for 1 hour. The beads were collected by centrifugation and washed twice with immunoprecipitation buffer, twice with high-salt immunoprecipitation buffer [500 mmol/L NaCl, 5 mmol/L EDTA, 1% Triton X-100, 0.5% NP40, 50 mmol/L Tris-HCl (pH 7.5), 0.5 mmol/L DTT], twice with stringent wash buffer [10 mmol/L Tris-HCl (pH 7.5), 0.25 mol/L LiCl, 0.5% NP40, 0.5% sodium deoxycholate, 1 mmol/L EDTA], and twice with TE buffer (10 mmol/L Tris-HCl, 0.1 mmol/L EDTA). The bound fraction was eluted in elution buffer (TE with 1% SDS) at 65°C for 10 minutes. Cross-links were reversed by incubating the eluate at 65°C for 6 hours. Samples were treated with proteinase K at 45°C for 1 hour, phenol/chloroform extracted, and ethanol precipitated. The primer sets used in PCRs are listed in Supplementary Table S2. PCRs were done on sample aliquots using denaturation at 95°C for 3 minutes followed by 35 cycles of 95°C for 30 seconds, 59°C for 45 seconds, and 72°C for 30 seconds. qrtPCR amplification of the promoter regions was done with 3 μ L DNA using the indicated primers and iQ SYBR Green Supermix from Bio-Rad (Hercules, CA) following the manufacturer's instructions.

Dual-function tyrosine kinase inhibitor and ER inhibitor studies. Proliferating BT-474 cells were treated with 6 μ Mol/L *N*-[4-[(3-bromophenyl)amino]-6-quinazolonyl]-2-butyrylamide EKI-785 (CL-387,785, Calbiochem, San Diego, CA) as an irreversible dual-function erbB1/erbB2 tyrosine kinase inhibitor or with 25 μ Mol/L 4-(4-benzyloxyanilino)-6,7-dimethoxyquinazolinone (4557W, Calbiochem) as a reversible competitive inhibitor of erbB1/2. We did not control estrogen levels in either the medium or sera used for these experiments. mRNA was harvested from cells treated with the inhibitors or vehicle controls 72 hours after treatment and gene expression was assessed by qrtPCR. Proliferating MCF-7 or BT-474 cells in DMEM with 10% bovine growth serum were incubated with 100 nmol/L fulvestrant or vehicle control to evaluate its effects on the candidate genes. Effects of the inhibitors on cell proliferation were evaluated 72 hours after treatment using the MTT assay.

Results

Identification of genes that display distinguishable levels of expression in preinvasive and invasive tumors. To identify genes that promote progression of preinvasive tissues to invasive carcinomas, we compared mRNA expression in preinvasive and invasive lesions in mammary tissues isolated from the same mouse using LCM. By analyzing transgenic models of human breast cancer-expressing genes that are thought to fall in a single proliferation control pathway (*erbB2*, *ras*, and *cyclin D1*), we sought to identify genes that might complement or lie downstream of this pathway and contribute to tumor progression. We first identified genes that displayed >2-fold differences in expression between preinvasive and invasive tissues in all mice from all three genotypes examined in the arrays (as detailed in Table 1 legend). These array results were confirmed by comparing qrtPCRs of the aRNAs used in

the arrays. We then compared changes in expression of the genes using qrtPCR of bulk normal mammary tissues, cyclin D1-induced preinvasive tissues, cyclin D1-induced tumors, and erbB2-induced tumors. Table 1 shows the fold changes in expression of the three genes (*E2-SSP1*, the immediate early response gene *IEX-1*, and *TRAF-IP*) that showed significant differences between murine cyclin D1 tumors and normal controls and between murine erbB2 tumors and normal controls.

We previously used microarrays to analyze gene expression changes across different stages of human breast cancer in aRNAs from tissues LCM microdissected from normal, ADH, DCIS, and IDC lesions that were isolated from 36 individual patient-matched samples (5). Although we previously used microarrays, in this study, we used qrtPCR of the isolated aRNAs to analyze expression changes only for the candidate genes identified by the murine samples. Of these, the same three genes displayed statistically significant changes in expression during carcinogenesis and cancer progression in human lesions as were found in mice (Table 1). Expression changes in these three genes are plotted for individual tumors in Supplementary Fig. S1, which presents scatter plots for the fold changes comparing tumor-normal and tumor-hyperplasia pairs. These genes increased ubiquitously in all murine tumors studied. The increases were progressive from preinvasive to invasive tumors.

We then used a separate set of human breast cancers to independently validate the role of these three genes in breast carcinogenesis (29). Using this alternative set of tumors, *E2-SSP1* increased 2.3 \pm 0.7-fold ($P = 0.001$, *t* test), *IEX-1* increased 3.8 \pm 0.7-fold ($P = 6.5 \times 10^{-7}$), and *TRAF-IP* increased 2.7 \pm 0.7-fold ($P = 0.001$) in breast cancers.

Functional analysis of genes up-regulated in breast tumors.

To examine their biological activities, we evaluated the effects of ectopic expression of *E2-SSP1*, *TRAF-IP*, and *IEX-1* in cell-based assays. As expected for genes involved in carcinogenesis and progression, *E2-SSP1*, *TRAF-IP*, and *IEX-1* promoted colony formation in soft agar assays (Fig. 1). When NIH3T3 transfectants were tested quantitatively for enhanced growth in soft agar colony assays, all three genes promoted anchorage-independent growth on their own (Fig. 1A). We also examined all three genes in MCF-10A cells that express an inducible variant of erbB2 that can be activated with a small molecule, AP1510, thus allowing us to examine collaborative effects of erbB2. All three genes promoted soft agar colony formation in the absence of erbB2 activation and synergistically enhanced soft agar colony formation in collaboration with erbB2 homodimerization (Fig. 1B).

We tested the effects of *E2-SSP1*, *TRAF-IP*, and *IEX-1* on cell proliferation and apoptosis to examine possible mechanisms underlying their effects on carcinogenesis. All three genes increased proliferation of transfected T47D (Fig. 1C) and MCF-7 cells (Fig. 1D). It seemed probable that this increased proliferation rate resulted from suppression of apoptosis because transfected cells accumulated faster without evident changes in S-phase entry. We therefore tested all three genes for antiapoptotic activity in MCF-7 and T47D using growth factor withdrawal and treatment with a death ligand to induce apoptosis. Cell death was decreased from a baseline of 18.0 \pm 3.4% apoptotic cells in MCF-7 cells to 9.7 \pm 3.9% by *IEX-1S*, 10.9 \pm 4.0% by *IEX-1L*, 10.3 \pm 3.9% by *E2-SSP1*, and 11.2 \pm 2.0% by *TRAF-IP* after growth factor removal. ($P < 0.05$, *t* test; graphs presented in Supplementary Fig. S2) The three genes decreased apoptosis in MCF-7 cells treated with TNF- α from 16.2 \pm 1.9% to 10.2 \pm 1.8% by *IEX-1S*, 6.9 \pm 1.3% by *IEX-1L*,

Table 1. Gene expression changes in tumor progression

Murine samples								
Gene name	Fold increase in arrays ($n = 6$)	Real-time D1 hyperplasia/normal ($n = 3$)	P , Student's t test	Real-time D1 tumor/normal ($n = 6$)	P , Student's t test	Real-time erbB2 tumor/normal ($n = 14$)	P , Student's t test	
<i>E2-SSP1</i>	2.82	4.04 ± 0.042	0.00043	69.8 ± 1.86	0.0695	12.1 ± 0.067	0.00936	
<i>IEX-1</i>	4.18	2.49 ± 0.038	0.0335	43.2 ± 0.714	0.0153	437.5 ± 1.16	1.08×10^{-5}	
<i>TRAF-IP</i>	2.31	19.2 ± 2.26	—	65.0 ± 0.358	1.02×10^{-4}	92.6 ± 0.236	1.08×10^{-5}	
Human samples								
Gene name	Real-time DCIS-ADH/normal	n	P , Student's t test	Real-time IDC/normal	n	P , Student's t test	Real-time IDC/DCIS-ADH	n
<i>E2-SSP1</i>	11.4 ± 3.60	42	0.00554	25.1 ± 3.6	27	0.034	7.87 ± 5.61	27
<i>IEX-1</i>	3.18 ± 0.81	42	0.00982	4.32 ± 0.80	27	0.00952	2.77 ± 0.88	27
<i>TRAF-IP</i>	1.95 ± 0.25	42	0.000353	2.75 ± 0.25	27	0.00118	1.43 ± 0.20	27

NOTE: Array fold change was calculated as the mean of 12 independent microarrays, which were done on six mice, and each array was done in duplicate. Ratios of hyperplasia/normal and tumor/normal and ratios of DCIS/normal, IDC/normal, and IDC/DCIS in human samples were calculated using the values from real-time qrtPCR for each tissue or tumor type. No erbB2 mouse ever developed bulk preinvasive tissues that could be distinguished from tumor tissue so no erbB2 hyperplasia data are presented. Shown are the mean \pm SE for the indicated tissues. Genes shown include *E2-SSP1*, the immediate early response-3 gene *IEX-1*, and *TRAF-IP*. In the initial arrays, the genes that displayed >2-fold differences in expression between preinvasive and invasive tissues in all mice from all three genotypes included the following: (a) *E2-SSP1* (HSPB8, HSP22), (b) *IEX-1*, (c) *TRAF-IP*, (d) *tescalcin*, (e) *Bruton's tyrosine kinase (BTK)*, (f) *cytidine monophospho-N-acetylneuraminic acid synthetase (CMAS)*, (g) melanoma-related gene-1 (*cited-2*), (h) *CGI55*, (i) *cadherin-1*, (j) milk fat globule-epidermal growth factor 8 protein (*lactadherin*), (k) *adipsin*, (l) *E2 ubiquitin-conjugating enzyme (E2UCE)*, and (m) *S-acyl fatty acid synthase thioesterase (SAFAT)*. Three genes (*lactadherin*, *adipsin*, and *E2UCE*) were down-regulated in the mouse array results but up-regulated in the murine bulk tumors and were therefore not further analyzed. *Tescalcin* was significantly increased in mice tumors but was significantly decreased in the human tumors. Differences in expression between preinvasive and invasive tissues for five genes, including *BTK*, *CMAS*, *cited-2*, *CGI55*, and *cadherin-1*, failed to show statistically significant differences in either the bulk murine tumor tissues or in the human LCM-isolated samples. *SAFAT* decreased significantly during murine tumor progression, similar to the reported changes in the human breast cancer-associated fatty acid synthase (49). However, *SAFAT* was only expressed in five normal human tissues and is known to function in milk production. It was therefore not further analyzed.

$4.5 \pm 1.3\%$ by *E2-SSP1*, and $11.2 \pm 2.1\%$ by *TRAF-IP* ($P < 0.05$, t test for all genes). The candidate genes also blocked apoptosis in T47D transfectants using growth factor removal or FAS ligand to provoke apoptosis (shown in Supplementary Fig. S2).

Regulation of candidate progression genes in response to cyclin D1 expression and to estrogen stimulation. Transgene expression frequently increases in transgenic tumors. This phenomenon is shown here for MMTV-cyclin D1 mice (Fig. 2A). We therefore considered that cyclin D1 might up-regulate the candidate genes. Using qrtPCR to measure mRNA levels in MCF-7 cells transfected with a control vector or cyclin D1, *E2-SSP1* mRNA increased 23.3-fold in MCF-7 cells stably transfected with cyclin D1 (Fig. 2B). *IEX-1* increased by 77% and *TRAF-IP* increased by 64% in response to cyclin D1. We were particularly interested in this regulation by cyclin D1 because cyclin D1 is associated with ER-positive tumors, and the *E2-SSP1* gene is highly responsive to 17β -estradiol (36). We therefore evaluated the estrogen regulation of all three progression genes using MCF-7 (BUS) cells (35) and found dose-dependent 17β -estradiol stimulation of *E2-SSP1*, *IEX-1*, and *TRAF-IP* (Fig. 2C). Finally, we used Western blots to show that all of the tumors found in the MMTV-cyclin D1 mice expressed the ER, an important finding in mouse models of human breast cancer (Fig. 2D).

To better understand the mechanisms underlying cyclin D1 and 17β -estradiol regulation of the candidate genes, we transfected MCF-7 cells with two additional mutant forms of cyclin D1. The KE mutant of cyclin D1 cannot interact with CDK4 and therefore cannot phosphorylate pRb (37). The LALA mutant of cyclin D1 lacks a steroid coactivator interaction domain and cannot activate EREs (23). These constructs were transfected into pooled MCF-7 cell transfectants. Using qrtPCR, changes in *E2-SSP1* mRNA were then evaluated in the four types of transfectants, in the absence and presence of 17β -estradiol. *E2-SSP1* expression increased >20-fold in cells expressing the KE mutant (Fig. 3A); the effect of cyclin D1 was blunted using the LALA mutant. We then evaluated *E2-SSP1* expression in both the absence (Fig. 3A, *white columns*) and presence (Fig. 3A, *black columns*) of 17β -estradiol in the various transfectants. 17β -Estradiol increased *E2-SSP1* mRNA ~4-fold in the control cells and magnified cyclin D1-induced changes in the cyclin D1 and KE transfectants. Estrogen treatments with the LALA mutant of cyclin D1 had smaller effects.

Cyclin D1, 17β -estradiol, and the cyclin D1- 17β -estradiol combination had similar but smaller effects on *IEX-1* and *TRAF-IP*. *IEX-1* mRNA increased in response to cyclin D1, its mutants, and combinations with 17β -estradiol (Fig. 4A). *TRAF-IP* mRNA increased in response to cyclin D1 and its mutants (Fig. 4B) but

was less 17 β -estradiol responsive in these transfectants than previously observed in the untransfected MCF-7 BUS cells (Fig. 2C), perhaps due to the multiple passages required during transfections.

Cyclin D1 and estrogen increase ER and CBP binding at the candidate gene promoters in chromatin immunoprecipitation experiments. We did chromatin immunoprecipitations (ChIP) to determine whether these responses to 17 β -estradiol and cyclin D1 resulted from changes in genomic ER binding to the E2-SSP1 promoter (Fig. 3B and C). We used quantitative ChIPs for ER and p300/CBP in the absence and presence of 17 β -estradiol. ER binding to the E2-SSP1 promoter increased markedly in response to both 17 β -estradiol treatment and cyclin D1 expression (Fig. 3B). This binding increased further in response to the combination of 17 β -estradiol and cyclin D1. Cyclin D1 expression also increased the binding of CBP to the E2-SSP1 promoter (Fig. 3C). We further found that cyclin D1 increased both ER and CBP binding at the IEX-1 promoter (Fig. 4C) and TRAF-IP promoters (Fig. 4D).

Inhibition of erbB2 receptor signaling down-regulates expression of the candidate genes. We originally sought to find genes that either complement or lie downstream of the *erbB2* \rightarrow *cyclin D1* pathway by identifying mRNAs that increased in invasive mammary lesions from *erbB2* and cyclin D1 transgenics. As

expected, *erbB2* is indeed increased in transgenic *erbB2* tumors (Fig. 5A). To investigate the role of *erbB2* as a potential regulator of the candidate genes, we therefore treated BT-474 cells, which overexpress *erbB1* and *erbB2*, with an irreversible dual kinase inhibitor of *erbB1/erbB2* signaling (CL-387,785). TRAF-IP, E2-SSP1, and IEX-1 mRNAs all decreased after treatment with this inhibitor (Fig. 5B).

The development of endocrine therapy resistance is a critical issue in breast cancer therapy and increasing data suggest that hormone therapy-resistant tumors become dependent on growth factor signaling (38, 39). We evaluated BT-474 cells, which are also ER positive, because combinations of dual kinase inhibitors and hormonal therapy are promising therapies for use to prevent hormone therapy resistance (40). We therefore examined the response of TRAF-IP, E2-SSP1, and IEX-1 to fulvestrant and combinations with either the irreversible dual kinase inhibitor or a reversible competitive dual kinase inhibitor (4557W; Fig. 5C). Fulvestrant (100 nmol/L) effects on the three genes varied somewhat among cell lines. E2-SSP1 mRNA fell to $10.1 \pm 0.4\%$, IEX-1 mRNA fell to $47.9 \pm 3.7\%$, and TRAF-IP mRNA fell to $17.5 \pm 0.6\%$ of their pretreatment levels after fulvestrant treatment of MCF-7 cells (data not graphed). Fulvestrant decreased E2-SSP1

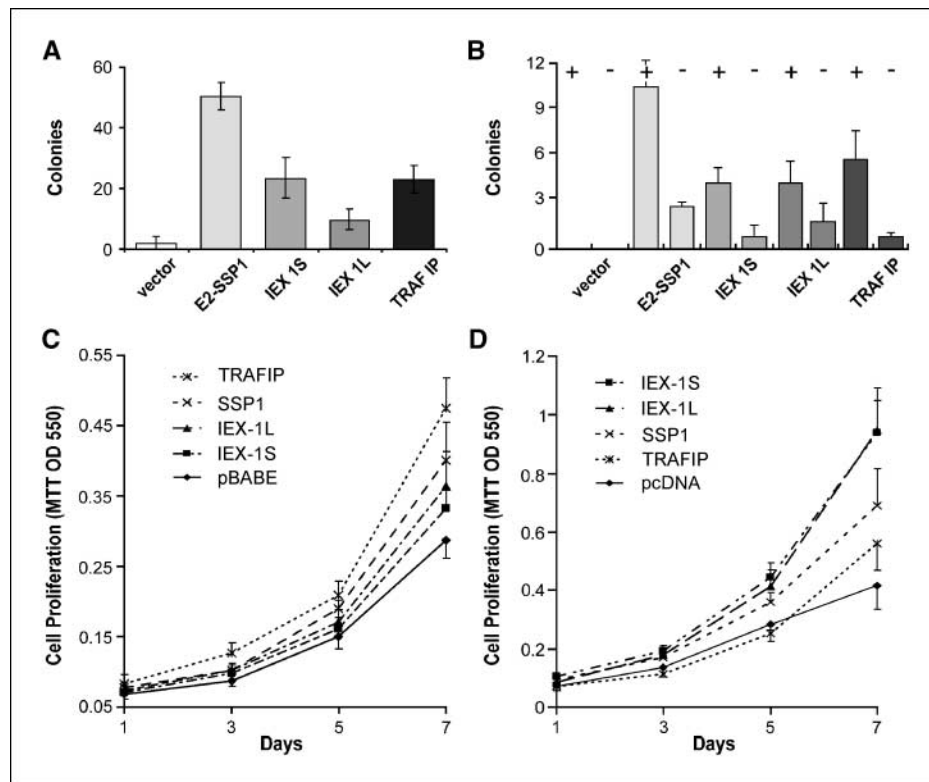


Figure 1. Transforming potential and effects on cell proliferation of three candidate breast cancer progression genes. **A**, counts of soft agar colonies in NIH3T3 cells stably transfected with genes of interest. The number of soft agar colonies found per well for NIH3T3 cells transfected with the indicated expression constructs 2 weeks after plating 3×10^4 cells (in the absence of antibiotic selection). Columns, mean of three wells in a six-well plate; bars, SE. **B**, soft agar colony formation in MCF-10A cells transfected with retroviruses expressing no insert (vector), IEX-1S, IEX-1L, E2-SSP1, and TRAF-IP was evaluated. Counts of soft agar colonies in MCF-10A transfectants in the presence (left column marked with +) or absence of *erbB2* dimerization (right column marked with -) were determined. The number of soft agar colonies found per well for MCF-10A cells infected with the indicated retroviral constructs 2 weeks after plating 5×10^4 cells (in the absence of antibiotic selection). Columns, mean of four wells; bars, SE. In this assay, *erbB2* alone did not induce colonies. **C**, enhanced proliferation rates in T47D cells stably overexpressing three candidate breast cancer progression genes. Points, mean of the A_{550} values for 10 wells stained with MTT to determine relative cell numbers at the indicated days (X axis); bars, SD. pBABE expression constructs were used to obtain T47D cells overexpressing IEX-1S, IEX-1L, E2-SSP1, TRAF-IP, and a vector control (pBABE). E2-SSP1, IEX-1L, and TRAF-IP, $P < 0.02$ on days 5 and 7 by *t* test compared with vector control. IEX-1S, $P < 0.05$ on day 7. **D**, enhanced proliferation rates in MCF-7 cells stably overexpressing three candidate breast cancer progression genes. Points, mean of the A_{550} values for 10 wells stained with MTT to determine relative cell numbers at the indicated days (X axis); bars, SD. pcDNA expression constructs were used to obtain MCF-7 cells overexpressing IEX-1S, IEX-1L, E2-SSP1, TRAF-IP, and a vector control (pcDNA). E2-SSP1, IEX-1L, and IEX-1S, $P < 0.01$ on days 3, 5, and 7 by ANOVA compared with vector control. TRAF-IP, $P = 0.27$ and 0.35 on days 5 and 7, respectively.

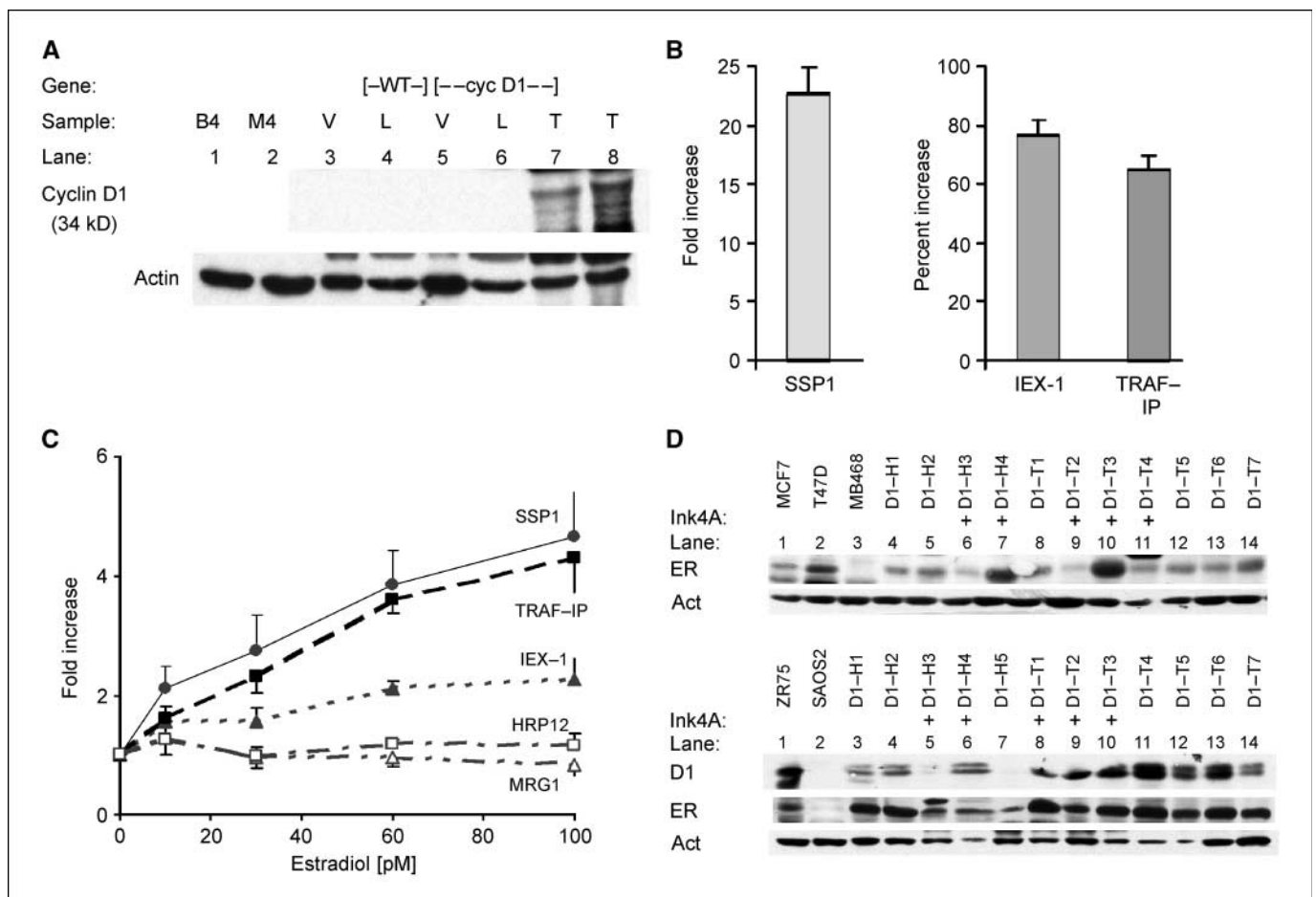


Figure 2. Candidate gene regulation by cyclin D1 and estrogen. **A**, Western blots for cyclin D1 show increased levels of the transgene-specific protein in tumors that arise in the MMTV-cyclin D1 mice. Control cell lines included BT-474 (B4) and MDA-MB-453 (M4). Virgin (V) and lactating (L) tissues were included as preneoplastic controls. Two tumors (T) were included to assess increased expression of the cyclin D1 transgene. Actin loading control. **B**, MCF-7 cells were transfected with a control vector or pCMV-cyclin D1. Pooled transfectants were selected in G418, and mRNA and protein harvested from confluent cells showed overexpression of the transfected cyclin D1 (data not shown). Expression of the three candidate progression gene mRNAs increased in response to cyclin D1 comparing fold increases in candidate mRNAs between the cyclin D1 transfectants and the vector-transfected controls. Columns, mean increase of three determinations; bars, SD. Y axis, fold or percentage change. The reverse-transcribed cDNA for all samples was measured on a fluorometer and each qRT-PCR was carried out using identical amounts of cDNA. **C**, 17 β -Estradiol induced expression of E2-SSP1, TRAF-IP, and IEX-1 in MCF-7 BUS cells. Fold increases in mRNA levels measured by qRT-PCR compared with no addition of 17 β -estradiol in cells continuously proliferating in the indicated concentrations of 17 β -estradiol. Expression of the indicated mRNAs. Points, mean of six determinations at each point; bars, SE. X axis, 17 β -estradiol concentration in picomolar; Y axis, fold increase when compared with the vehicle-treated cells. **D**, mammary tumors in MMTV-cyclin D1 transgenic mice are ER positive. Western blots for ER, cyclin D1 (D1), and actin (Act). We used two different antibodies to the ER in the two different blots. Samples are from MMTV-cyclin D1 hyperplasia (D1-H#) and tumor tissues (D1-T#). Tumor samples are identical between the top two rows and the bottom three rows. We used MCF-7 and T47D cells as positive controls for ER (top row) and compared them to MB468 as a negative control. D1-H, cyclin D1 transgenic hyperplasia mammary tissue; D1-T, cyclin D1 transgenic mammary tumors. We used ZR75 as a positive control for ER and cyclin D1 compared with SAOS2 as a negative control (third and fourth rows) for both genes.

mRNA to 10% and TRAF-IP mRNA to 74% of their pretreatment levels in BT-474 cells (Fig. 5C). For unclear reasons that may be related to cell-specific interactions between ER and erbB1 signaling, fulvestrant increased IEX-1 mRNA in this cell line. The competitive dual kinase inhibitor 4557W (25 μ M/L) decreased both TRAF-IP and IEX-1 mRNAs to a similar extent as CL-387,785 (6 μ M/L) but was not as effective in decreasing E2-SSP1. When 100 nmol/L fulvestrant was combined with either inhibitor, however, TRAF-IP, E2-SSP1, and TRAF-IP mRNAs fell more than when the cells were treated with the kinase inhibitors alone. Combinations of CL-387,785 with fulvestrant may be more meaningful for TRAF-IP and IEX-1 because fulvestrant alone was more effective than the combinations in reducing E2-SSP1 levels. Finally, we confirmed that at these doses the combination of fulvestrant with the dual kinase inhibitors had stronger effects on BT-474 cell proliferation (Fig. 5D).

Discussion

Breast cancer progression genes. By identifying genes whose expression increased as tumor invasion progressed, we distinguished three genes that were associated with the histologic changes accompanying cancer progression. IEX-1 (NM 133662) was initially found as a radiation-inducible protein in squamous carcinomas (41). It blocks apoptosis and causes T-cell lymphomas in transgenic mice (42). TRAF-IP (NM 011634) is a novel component of the TNF receptor signaling complex that inhibits TNF-induced nuclear factor- κ B (NF- κ B) activation but not interleukin-1-induced NF- κ B activation (43). E2-SSP1 was identified as SSP (NM 030704, HSPB8; ref. 36), which transformed tissue culture cells. Its isolation as a target gene of estrogen action led us to term it a E2-SSP1 (36). Our results confirm that all three genes have relatively weak transforming activities that are magnified by collaboration with erbB2 (Fig. 1).

Transgenic models have guided many perspectives about the nature of cooperating events in tumor progression. Collaborating events have been confirmed using genetic crosses (9). DNA microarray technology has been used to identify gene expression signatures in mouse models (44). Using arrays to identify candidate genes, we sought to identify changes in invasive breast cancers that might result from progressive quantitative changes in gene expression. To provide the best chance to identify genes relevant to human breast cancer, we focused our studies on a signaling pathway important in human breast cancer (11, 25). Through microarray analysis and qrtPCR, we identified three candidate genes (Table 1).

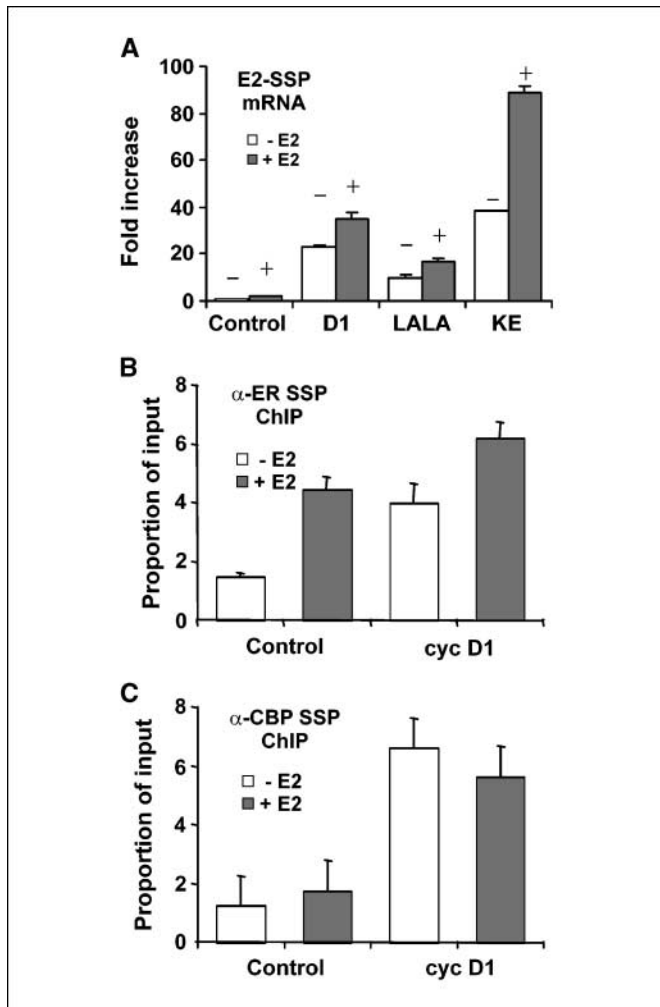


Figure 3. E2-SSP1 gene regulation by cyclin D1 and estrogen. *A*, expression of E2-SSP1 mRNA increases in response to cyclin D1 and to estrogen. MCF-7 cells were transfected with a control vector (*Vector*), pCMV-cyclin D1, pCMV-cyclin D1 mutant KE (*KE*), and pCMV mutant LALA (*LALA*). Pooled transfectants were selected in G418, and mRNA and protein were harvested from confluent cells to evaluate expression of the transfectants. mRNA was harvested from the indicated transfectants in the absence (*white columns* marked with $-$) and presence (*black columns* marked with $+$) of 17β -estradiol as described in Materials and Methods. *Columns*, mean of three determinations; *bars*, SD. We used qrtPCR to assess fold increases in expression of E2-SSP1; *Y axis*, fold change. The reverse-transcribed cDNA for all samples was measured on a fluorometer and each qrtPCR was carried out using identical amounts of cDNA. *B* and *C*, ChIP was carried out using nonimmune serum, anti-ER (α -ER; *B*), and anti-CBP (α -CBP; *C*) as described in Materials and Methods. Immunoprecipitations were done in the absence (*white columns*) and presence (*black columns*) of 17β -estradiol. Nonimmune serum generated no signal. *Columns*, mean of triplicate samples shown as a percentage of input; *bars*, SD. ChIP assays were done for vector control-transfected cells (*Control*) and cells transfected with cyclin D1 (*cyc D1*).

We then extended our analysis to human samples to evaluate whether any candidates might be relevant to human disease.

The histology of murine transgenic tumors strongly mimics the appearance of human tumors expressing human breast cancer genes used to generate the models (8). To assess the degree to which murine models also model the molecular pathogenesis of specific human tumor types, we focused on a comparison of erbB2- and cyclin D1-driven models and disease. Interestingly, the carcinogenesis and progression genes identified in our screen identified both general progression events and specific pathogenic events in cyclin D1- and erbB2-driven tumors. The initial increases in expression of the three genes from normal murine to hyperplastic tissues (E2-SSP1, 4.0-fold; IEX-1, 2.5-fold; and TRAF-IP, 19-fold) were magnified when tumors were compared with normal controls (70-, 43-, and 65-fold) in the cyclin D1 model. Comparing the change from normal human to DCIS with the change from DCIS to IDC, the E2-SSP1 increased first 11-fold and then another 8-fold, IEX-1 first increased 3.2-fold and then another 2.8-fold, and the TRAF-IP first increased 1.95-fold and then another 1.4-fold. Importantly, E2-SSP1 showed the most specific response to cyclin D1 and erbB2 because its increase was only 11.6 ± 5.2 -fold in cyclin D1- and erbB2-negative tumors but became 22.4 ± 7.5 -fold in cyclin D1-positive tumors, 30.6 ± 11.1 -fold in cyclin D1/ER-positive tumors, and 20.8 ± 9.7 -fold in erbB2-positive tumors. IEX-1 increased 1.6 ± 0.4 -fold in cyclin D1- and erbB2-negative tumors but became 3.7 ± 0.8 -fold in cyclin D1-positive tumors, 4.6 ± 1.2 -fold in cyclin D1/ER-positive tumors, and 4.0 ± 0.7 -fold in erbB2-positive tumors. TRAF-IP did not show significant relationships with cyclin D1 or erbB2, perhaps because the magnitude of its change was less than the other two genes. Obviously, these three genes are not likely to be the only genes involved in breast cancer progression because we analyzed only the named genes in arrays that contained an incomplete set of mouse cDNAs. It is probably not surprising that the genetic changes we found in the human tumors did not precisely match all of the events identified in the mouse model tumors given the greater complexity of the genetic events contributing to the human cancers. However, it is remarkable that we identified previously undiscovered endogenous targets of the proposed molecular interaction between cyclin D1 and the ER that was first proposed in human cells.

The identity of the genes we found agree with a view that acquisition of resistance to apoptosis may be a particularly important step in cancer progression (45). Proliferative oncogenic signals like those used in our mouse models, including erbB2, ras, and cyclin D1, simultaneously act as potent activators of cell death (45, 46). Coupling of their oncogenic signals to the death apparatus usually serves to check neoplastic development in normal cells. It is therefore not unexpected that all three genes displayed antiapoptotic functions.

Regulation of breast cancer progression genes. We initially evaluated *erbB2*, *ras*, and *cyclin D1* transgenic mice to identify oncogenic events that might complement or fall downstream of the proposed *erbB2* \rightarrow cyclin D1 signaling pathway. Importantly, expression of all three candidates increased in association with increased erbB2 and/or cyclin D1 in our human tumors (Table 1). Thus, selection for the driving event in oncogenesis likely drives some of the increased expression of these cancer progression genes.

Estrogen response was a second event regulating expression of our cancer progression genes (Fig. 2C). The prevalence of ER-positive tumors in our patient samples might have contributed to our identification of ER-responsive genes because 80% of

the human neoplasias (DCIS-ADH plus IDC) studied were ER positive. Moreover, we have now shown that murine MMTV-cyclin D1-induced tumors are ER positive (Fig. 2D). The combination of screening in both cyclin D1-driven tumors and these particular human samples probably contributed to our identification of genes regulated in response to both cyclin D1 and ER. Importantly, although the association of cyclin D1 and ER is well described, endogenous target genes of both have never been identified previously. This result suggests the important possibility that selection for the combination of cyclin D1 and the ER causes a more invasive phenotype than expression of ER alone, which might also explain the association between cyclin D1 and the development of invasive characteristics (17).

Why is cyclin D1 overexpression associated with ER-positive breast cancers? Overexpression of cyclin D1 is associated with ER-positive breast cancers (16, 19). Remarkably, despite CDK4-dependent phosphorylation of pRb by cyclin D1, CDK activity is not increased in breast cancer (47). We were therefore quite interested to find out that our genes responded to both estrogen stimulation and cyclin D1, as expected if cyclin D1 indeed interacts with coactivators of the ER (21–23). Interactions between cyclin D1 and the ER were first suggested when transfected cyclin D1 was shown to induce ERE-driven reporter gene expression (21, 22). This induction was independent of both CDK4 and estrogen ligand and depended on direct protein interactions between cyclin D1 and either the steroid coactivator-1 or the p300/CBP-binding protein

associated protein (23, 48). Importantly, a mutation (the LALA mutant) in a leucine-rich motif in cyclin D1 blocks activation of the ERE by cyclin D1(23).

Our results are consistent with this proposed interaction between cyclin D1 and the steroid coactivator apparatus. Cyclin D1 expression uniformly enhanced p300 coactivator binding to the E2-SSP1, IEX-1, and TRAF-IP promoters (Figs. 3 and 4). Cyclin D1 increased expression of all three genes (Fig. 2B). Importantly, although estrogen induced expression of all three genes, its effects occurred independently of the effects of cyclin D1 as would be predicted by the previous ligand independence of the effects of cyclin D1 on the ERE. Finally, the LALA mutant was less active in stimulating candidate gene expression and the KE mutant was more active than cyclin D1 in stimulating E2-SSP1 expression. Our results provide important biological support for the D1-steroid coactivator model and suggest that it is a meaningful function of cyclin D1 in invasive breast cancer.

Finally, with the identification of genes that are associated with the histologic acquisition of invasive characteristics, inhibitory strategies will be needed to prove their potential as therapeutic targets. Genes that are regulated by growth factors and the ER would be of considerable therapeutic interest as trials of combination tyrosine kinase inhibitors and ER inhibitors are initiated (38, 39). It remains to be determined if the combination of IEX-1, E2-SSP1, and TRAF-IP augment each other's functions in breast cancer progression. However, these studies have revealed important

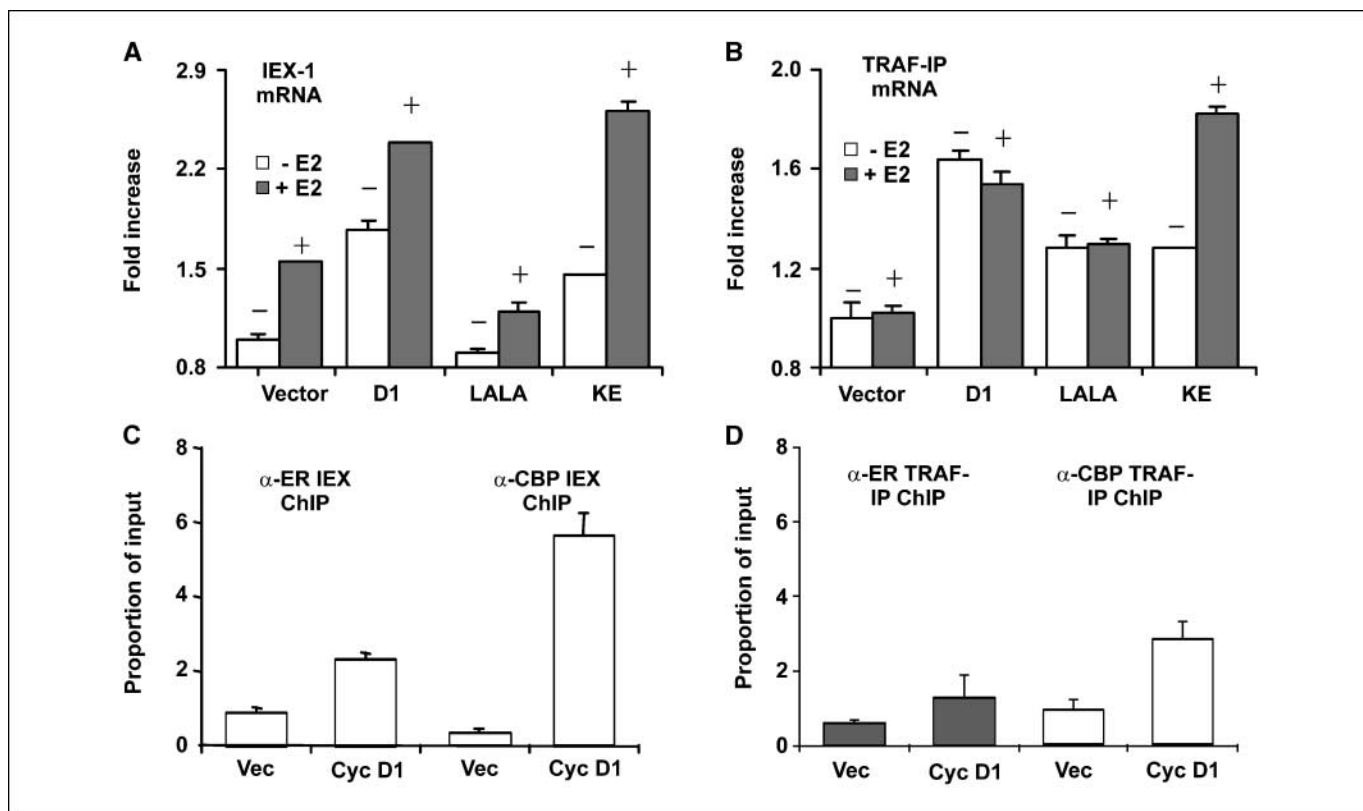


Figure 4. IEX-1 and TRAF-IP mRNAs are regulated by 17 β -estradiol and cyclin D1. *A* and *B*, MCF-7 cells transfected with control vector, pCMV-cyclin D1, pCMV-cyclin D1 mutant KE, and pCMV mutant LALA. mRNA was harvested from the cyclin D1 transfectants in the absence (*white columns* marked with $-$) and presence (*black columns* marked with $+$) of 17 β -estradiol. *Columns*, mean of three determinations; *bars*, SD. We used qrtPCR to assess fold increases in expression of IEX-1 (*A*) and TRAF-IP (*B*) mRNAs. *Y axis*, fold change. *C* and *D*, ChIP was carried out using nonimmune serum, anti-ER (α -ER), and anti-CBP (α -CBP) as described in Materials and Methods. Nonimmune serum generated no signal. *Columns*, mean of triplicate samples shown as a percentage of input; *bars*, SD. ChIP assays were done for vector control-transfected cells (*Vec*) and cells transfected with cyclin D1. qrtPCR assessed ER and CBP binding to the IEX-1 (*C*) and TRAF-IP (*D*) promoters.

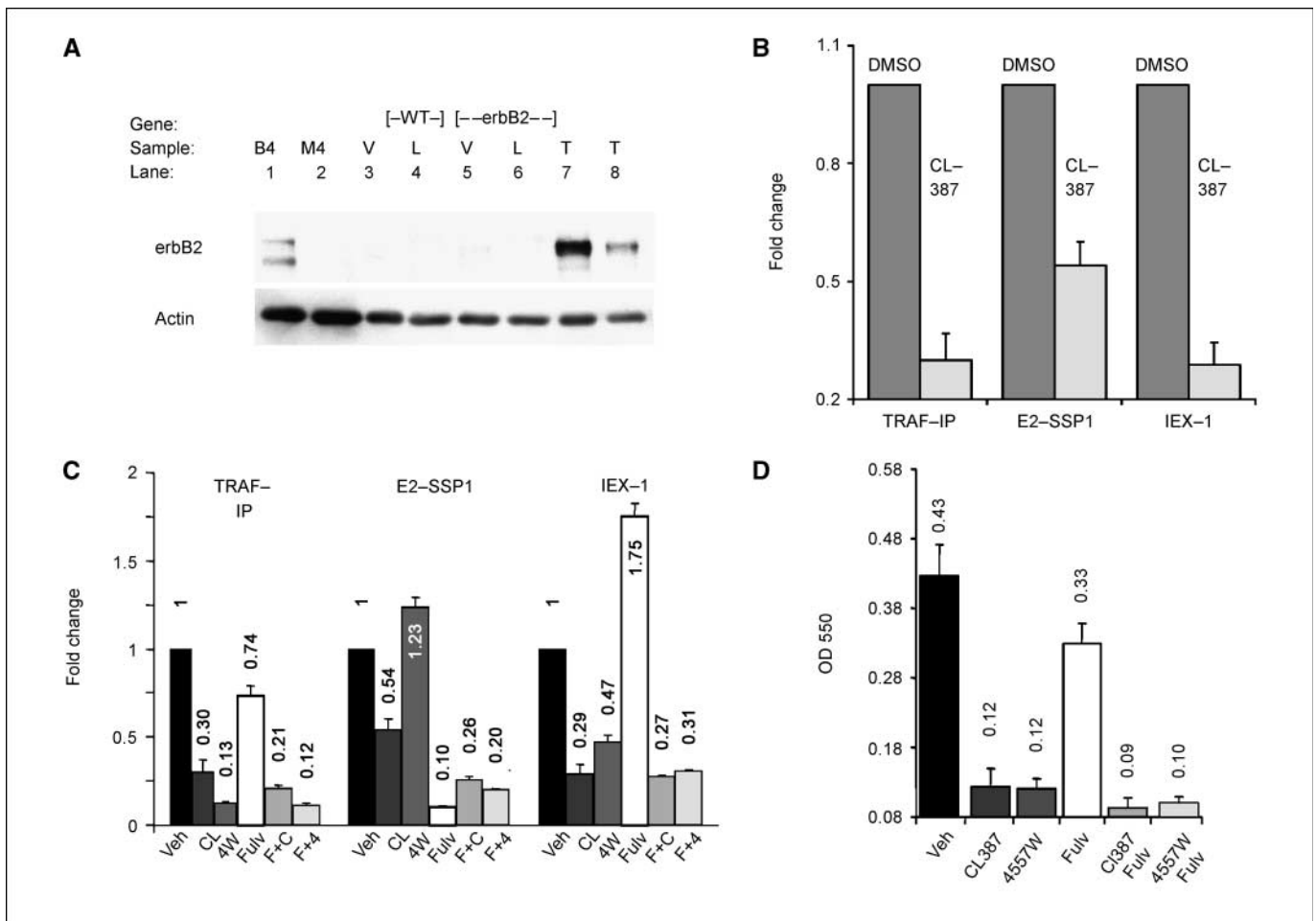


Figure 5. Inhibitors of erbB1 and erbB2 decrease TRAF-IP, E2-SSP1, and IEX-1 gene expression. **A.** Western blots for erbB2 show increased levels of the erbB2 transgene in tumors that arise in the MMTV-erbB2 mice. Control cell lines included BT-474 and MDA-MB-453. Virgin and lactating tissues were included as preneoplastic controls. Two tumors from the erbB2 transgenic strain were included to assess increased expression of erbB2 protein. An actin loading control is shown for each panel of samples. **B.** Proliferating BT-474 cells were treated with 6 $\mu\text{mol/L}$ CL-387,785 irreversible dual kinase inhibitor of erbB1/erbB2 signaling (CL-387) or vehicle control (DMSO) for 72 hours and mRNA was harvested. Expression levels of TRAF-IP, E2-SSP1, and IEX-1 mRNAs were determined using qRT-PCR. Columns, mean of fold changes comparing control samples with inhibitor-treated samples; bars, SD. **C.** Proliferating BT-474 cells were treated with 6 $\mu\text{mol/L}$ L-387,785 (CL), 25 $\mu\text{mol/L}$ 4557W reversible competitive dual kinase inhibitor (4W), 100 nmol/L fulvestrant (Fulv), combined 100 nmol/L fulvestrant plus 6 $\mu\text{mol/L}$ CL-387,785 (F + C), combined 100 nmol/L fulvestrant plus 25 $\mu\text{mol/L}$ 4557W (F + 4), or vehicle control (Veh) for 72 hours and mRNA was harvested. Expression levels of TRAF-IP, E2-SSP1, and IEX-1 mRNAs were determined using qRT-PCR. Columns, mean of fold changes comparing control samples with inhibitor-treated samples; bars, SD. **D.** Proliferating BT-474 cells were treated with 6 $\mu\text{mol/L}$ CL-387,785, 25 $\mu\text{mol/L}$ 4557W reversible competitive dual kinase inhibitor (4557W), 100 nmol/L fulvestrant, combined 100 nmol/L fulvestrant plus 6 $\mu\text{mol/L}$ CL-387,785 (CL387 + Fulv), combined 100 nmol/L fulvestrant plus 25 $\mu\text{mol/L}$ 4557W (4557W + Fulv), or vehicle control for 72 hours and cell numbers were evaluated with the MTT assay. A_{550} measurement of cell numbers. Columns, mean of 10 determinations at each point; bars, SD.

targets of regulation by cyclin D1 and estrogen and have confirmed the value of simultaneously studying oncogenesis in humans and mouse models.

Acknowledgments

Received 5/4/2006; revised 8/1/2006; accepted 10/11/2006.

Grant support: NIH National Cancer Institute (NCI) grant R01 CA69069 (V. Ionescu-Tiba and E.V. Schmidt); Harvard Breast Cancer Specialized Programs

References

- Nowell PC. The clonal evolution of tumor cell populations. *Science* 1976;194:23-8.
- Sporn MB. The war on cancer. *Lancet* 1996;347:1377-81.
- Page DL, Jensen RA, Simpson JF, et al. Historical and epidemiologic background of human premalignant

breast disease. *J Mammary Gland Biol Neoplasia* 2000; 5:341-9.

- Porter DA, Krop IE, Nasser S, et al. A SAGE (serial analysis of gene expression) view of breast tumor progression. *Cancer Res* 2001;61:5697-702.
- Ma XJ, Salunga R, Tuggle JT, et al. Gene expression profiles of human breast cancer progression. *Proc Natl Acad Sci U S A* 2003;100:5974-9.
- Allinen M, Beroukhi R, Cai L, et al. Molecular characterization of the tumor microenvironment in breast cancer. *Cancer Cell* 2004;6:17-32.
- Mills JC, Roth KA, Cagan RL, et al. DNA microarrays and beyond: completing the journey from tissue to cell. *Nat Cell Biol* 2001;3:E175-8.
- Cardiff RD, Anver MR, Gusterson BA, et al. The mammary pathology of genetically engineered mice:

- the consensus report and recommendations from the Annapolis meeting. *Oncogene* 2000;19:968–88.
9. Sinn E, Muller W, Pattengale P, et al. Coexpression of MMTV/v-Ha-ras and MMTV/c-myc genes in transgenic mice: synergistic action of oncogenes *in vivo*. *Cell* 1987; 49:465–75.
 10. Sutherland RL, Musgrove EA. Cyclins and breast cancer. *J Mammary Gland Biol Neoplasia* 2004;9:95–104.
 11. Sicinski P, Donaher JL, Parker SB, et al. Cyclin D1 provides a link between development and oncogenesis in the retina and breast. *Cell* 1995;82:621–30.
 12. Wang TC, Cardiff RD, Zukerberg L, et al. Mammary hyperplasia and carcinoma in MMTV-cyclin D1 transgenic mice. *Nature* 1994;369:669–71.
 13. Dowdy SF, Hinds PW, Louie K, et al. Physical interaction of the retinoblastoma protein with human D cyclins. *Cell* 1993;73:499–511.
 14. LaBaer J, Garrett MD, Stevenson LF, et al. New functional activities for the p21 family of CDK inhibitors. *Genes Dev* 1997;11:847–62.
 15. Bernards R. CDK-independent activities of D type cyclins. *Biochim Biophys Acta* 1999;1424:M17–22.
 16. Zukerberg LR, Yang WI, Gadd M, et al. Cyclin D1 (PRAD1) protein expression in breast cancer: approximately one-third of infiltrating mammary carcinomas show overexpression of the cyclin D1 oncogene. *Mod Pathol* 1995;8:560–7.
 17. Weinstat-Saslow D, Merino MJ, Manrow RE, et al. Overexpression of cyclin D mRNA distinguishes invasive and *in situ* breast carcinomas from non-malignant lesions. *Nat Med* 1995;1:1257–60.
 18. Bieche I, Olivi M, Nagues C, et al. Prognostic value of CCND1 gene status in sporadic breast tumours, as determined by real-time quantitative PCR assays. *Br J Cancer* 2002;86:580–6.
 19. van Diest PJ, Michalides RJ, Jannink L, et al. Cyclin D1 expression in invasive breast cancer. Correlations and prognostic value. *Am J Pathol* 1997;150:705–11.
 20. Planas-Silva MD, Shang Y, Donaher JL, et al. AIB1 enhances estrogen-dependent induction of cyclin D1 expression. *Cancer Res* 2001;61:3858–62.
 21. Neuman E, Ladha MH, Lin N, et al. Cyclin D1 stimulation of estrogen receptor transcriptional activity independent of cdk4. *Mol Cell Biol* 1997;17: p5338–47.
 22. Zwijnen RM, Wientjens E, Klompaker R, et al. CDK-independent activation of estrogen receptor by cyclin D1. *Cell* 1997;88:405–15.
 23. Zwijnen RM, Buckle RS, Hijmans EM, et al. Ligand-independent recruitment of steroid receptor coactivators to estrogen receptor by cyclin D1. *Genes Dev* 1998; 12:p3488–98.
 24. Gadd M, Pisc C, Branda J, et al. Regulation of cyclin D1 and p16(INK4A) is critical for growth arrest during mammary involution. *Cancer Res* 2001;61:8811–9.
 25. Yang C, Ionescu-Tiba V, Burns K, et al. The role of the cyclin D1-dependent kinases in ErbB2-mediated breast cancer. *Am J Pathol* 2004;164:1031–8.
 26. Yu Q, Geng Y, Sicinski P. Specific protection against breast cancers by cyclin D1 ablation. *Nature* 2001;411: 1017–21.
 27. Lee RJ, Albanese C, Fu M, et al. Cyclin D1 is required for transformation by activated Neu and is induced through an E2F-dependent signaling pathway. *Mol Cell Biol* 2000;20:672–83.
 28. Zwicker J, Brusselbach S, Jooss KU, et al. Functional domains in cyclin D1: pRb-kinase activity is not essential for transformation. *Oncogene* 1999;18:19–25.
 29. Kawakubo H, Brachtel E, Hayashida T, et al. Loss of B-cell translocation gene-2 in estrogen receptor-positive breast carcinoma is associated with tumor grade and overexpression of cyclin d1 protein. *Cancer Res* 2006;66: 7075–82.
 30. Grushko TA, Dignam JJ, Das S, et al. MYC is amplified in BRCA1-associated breast cancers. *Clin Cancer Res* 2004;10:499–507.
 31. Muthuswamy SK, Li D, Lelievre S, et al. ErbB2, but not ErbB1, reinitiates proliferation and induces luminal repopulation in epithelial acini. *Nat Cell Biol* 2001;3: 785–92.
 32. Muthuswamy SK, Gilman M, Brugge JS. Controlled dimerization of ErbB receptors provides evidence for differential signaling by homo- and heterodimers. *Mol Cell Biol* 1999;19:6845–57.
 33. Carey JL, Sasur LM, Kawakubo H, et al. Mutually antagonistic effects of androgen and activin in the regulation of prostate cancer cell growth. *Mol Endocrinol* 2004;18:696–707.
 34. Qi XM, He H, Zhong H, et al. Baculovirus p35 and Z-VAD-fmk inhibit thapsigargin-induced apoptosis of breast cancer cells. *Oncogene* 1997;15:1207–12.
 35. Coser KR, Chesnes J, Hur J, et al. Global analysis of ligand sensitivity of estrogen inducible and suppressible genes in MCF-7/BUS breast cancer cells by DNA microarray. *Proc Natl Acad Sci U S A* 2003;100: 13994–9.
 36. Charpentier AH, Bednarek AK, Daniel RL, et al. Effects of estrogen on global gene expression: identification of novel targets of estrogen action. *Cancer Res* 2000;60:5977–83.
 37. Hinds PW, Dowdy SF, Eaton EN, et al. Function of a human cyclin gene as an oncogene. *Proc Natl Acad Sci U S A* 1994;91:709–13.
 38. Goss PE. Changing clinical practice: extending the benefits of adjuvant endocrine therapy in breast cancer. *Semin Oncol* 2004;31:15–22.
 39. Johnston SR. Combinations of endocrine and biological agents: present status of therapeutic and presurgical investigations. *Clin Cancer Res* 2005;11: 889–99s.
 40. Chu I, Blackwell K, Chen S, et al. The dual ErbB1/ErbB2 inhibitor, lapatinib (GW572016), cooperates with tamoxifen to inhibit both cell proliferation- and estrogen-dependent gene expression in antiestrogen-resistant breast cancer. *Cancer Res* 2005;65:18–25.
 41. Kondratyev AD, Chung KN, Jung MO. Identification and characterization of a radiation-inducible glycosylated human early-response gene. *Cancer Res* 1996;56: 1498–502.
 42. Zhang Y, Finegold MJ, Porteu F, et al. Development of T-cell lymphomas in Emu-IEX-1 mice. *Oncogene* 2003; 22:6845–51.
 43. Lee SY, Choi Y. TRAF-interacting protein (TRIP): a novel component of the tumor necrosis factor receptor (TNFR) and CD30-TRAF signaling complexes that inhibits TRAF2-mediated NF- κ B activation. *J Exp Med* 1997;185:1275–85.
 44. Fargiano AA, Desai KV, Green JE. Interrogating mouse mammary cancer models: insights from gene expression profiling. *J Mammary Gland Biol Neoplasia* 2003;8:321–34.
 45. Evan GI, Vousden KH. Proliferation, cell cycle, and apoptosis in cancer. *Nature* 2001;411:342–8.
 46. Weinstein EJ, Grimm S, Leder P. The oncogene heregulin induces apoptosis in breast epithelial cells and tumors. *Oncogene* 1998;17:2107–13.
 47. Sweeney KJ, Swarbrick A, Sutherland RL, et al. Lack of relationship between CDK activity and G₁ cyclin expression in breast cancer cells. *Oncogene* 1998;16: 2865–78.
 48. McMahon C, Suthiphongchai T, DiRenzo J, et al. P/CAF associates with cyclin D1 and potentiates its activation of the estrogen receptor. *Proc Natl Acad Sci U S A* 1999;96:5382–7.
 49. Alo PL, Visca P, Marci A, et al. Expression of fatty acid synthase (FAS) as a predictor of recurrence in stage I breast carcinoma patients. *Cancer* 1996;77:474–82.